

This is the peer reviewed version of the following article:

A composite cool colored tile for sloped roofs with high 'equivalent' solar reflectance / Ferrari, Chiara; Libbra, Antonio; Cernuschi, Federico Maria; De Maria, Letizia; Marchionna, Stefano; Barozzi, Matteo; Siligardi, Cristina; Muscio, Alberto. - In: ENERGY AND BUILDINGS. - ISSN 0378-7788. - STAMPA. - 114:(2016), pp. 221-226. [10.1016/j.enbuild.2015.06.062]

*Terms of use:*

The terms and conditions for the reuse of this version of the manuscript are specified in the publishing policy. For all terms of use and more information see the publisher's website.

16/05/2026 12:25

(Article begins on next page)

1 **A composite cool colored tile for sloped roofs**

2 **with high ‘equivalent’ solar reflectance**

3

4

5 Chiara Ferrari<sup>1</sup>, Antonio Libbra<sup>1</sup>, Federico Maria Cernuschi<sup>2</sup>, Letizia De Maria<sup>2</sup>, Stefano

6 Marchionna<sup>2</sup>, Matteo Barozzi<sup>3</sup>, Cristina Siligardi<sup>1</sup>, Alberto Muscio<sup>1,\*</sup>

7 <sup>1</sup>Univ. of Modena & Reggio Emilia (Italy), <sup>2</sup>RSE SpA (Italy), <sup>3</sup>Barozzi Vernici Srl (Italy)

8

9 \*Corresponding author: <sup>1</sup> Phone: +39 059 2056194; website: [www.eelab.unimore.it](http://www.eelab.unimore.it); email:

10 [alberto.muscio@unimore.it](mailto:alberto.muscio@unimore.it) (A. Muscio).

11

12

13 **KEYWORDS**

14 Cool roof, cool color, roof tile, solar reflectance, thermal transmittance

15

16

17 **HIGHLIGHTS**

- 18 • Ceramic tiles covers the roofs of Mediterranean cities.
- 19 • Their low solar reflectance can cause overheating of the built environment below.
- 20 • Cool colors can be exploited to achieve a higher reflectance.

- 21 • An equivalent, much higher, reflectance can be achieved by coupling with an aerogel layer  
22 and a radiant barrier.

23

## 24 **ABSTRACT**

25 Mediterranean cities are characterized by sloped roofs with ceramic tiles of traditional  
26 colors such as brick red in different tones. Their solar reflectance is generally low and can cause  
27 overheating of the building due to solar gains during the hot season.

28 In this work, an innovative approach is tested to achieve roof tiles with high capacity of  
29 rejecting solar radiation. It consists of using a cool-colored tile with relatively high solar  
30 reflectance, combined with a thin insulating layer attached below the tile and made of a silica-gel  
31 super-insulating material. An aluminum foil with very low thermal emittance is also applied  
32 below the insulating layer. Along the perimeter of each tile, line brushes are attached in order to  
33 enclose an almost sealed air space between the aluminum foil and the roof slab below when the  
34 tiles are supported on wooden battens.

35 Composite tiles like that outlined here can provide a strong increase of roof thermal  
36 resistance, helpful to control either heat loss in winter, or building overheating in summer. They  
37 can be installed onto an existing roof, for instance the sloped tile roof of a historical or traditional  
38 building, with no need to modify the roof height and structure.

## 39 **Introduction**

40 In the last decades the urban heat island (UHI) phenomenon more and more affected the  
41 temperature of urban areas, with a sensible increase of air temperature in comparison with the

42 surrounding rural areas. Both controllable and uncontrollable causes may origin UHI; among the  
43 latter ones anticyclone conditions, extremely hot seasons, sun intensity, wind speed and cloud  
44 cover can be found. Urban design and structure related variables (sky view factor, green areas,  
45 building materials), or population related variables (anthropogenic heat and air pollutants), are  
46 among controllable variables as reported by [1]. Several consequences are originated by the UHI,  
47 the most important ones being the significant change of climate, the increase of greenhouse gases  
48 and CO<sub>2</sub> emissions, and the increase of energy consumption of buildings due to the larger use of  
49 electricity for air conditioning.

50 In the last decades the attempt to reduce UHI stimulated the research of several solutions  
51 such as solar reflective surfaces [1]. The first studies were carried out since the late 90's when  
52 LBNL scientists started to analyze how high albedo materials can either mitigate UHI [2] or  
53 reduce energy use [3-4], as well as improve air quality [5]. Studies started in southern U.S., but  
54 they were then widened to consider different areas and climates [6]. More recently, in 2012,  
55 further analyses on the benefits related to reflective roofs and pavements use were made both in  
56 the US [7] and in Europe [8]. Along the years, several generations of cool roofing materials were  
57 implemented, as reported in Santamouris [9].

58 Not only the increase of solar reflective areas but also green surfaces such as green roofs  
59 were widely analyzed. Studies on the energy and environmental performance [10] and the  
60 surface heat budget [11] of green roofs were carried out more than a decade ago, also trying to  
61 establish models for building energy simulation programs [12]. More recently, investigations  
62 were made on building energy savings [13], pollution abatement [14] and mitigation potential

63 related to green roof in specific areas such as Chicago [15], tropical areas [16] and  
64 Mediterranean regions [17].

65 This work is focused on a new cool roof generation, characterized by high-reflectance  
66 coatings properly added with pigments that create the so called cool colors [18-19], that is  
67 colored surfaces with a high reflectivity in the infrared range of the solar spectrum [21-22].  
68 Recent studies on acrylic coatings [23-24] highlighted that not only the coating but also the  
69 substrate is crucial for the achievement of an adequate solar reflectance. Moreover, it was found  
70 that the use of a ceramic support for both clay roof tiles [24-25] and traditional porcelain  
71 stoneware tiles [26-27] can provide very high solar reflectance over the whole solar spectrum  
72 and high durability against time.

73 In this work, an innovative approach is tested to achieve roof tiles with high capacity of  
74 rejecting solar radiation. It consists of using a cool-colored red tile with common brick  
75 (terracotta) color but relatively high solar reflectance, coupled with a thin insulating layer  
76 attached below the tile and made of a silica-gel super-insulating material. An aluminum foil with  
77 very low thermal emittance is also applied below the insulating layer to act as radiant barrier.  
78 Along the perimeter of each tile, line brushes are attached in order to enclose an almost sealed air  
79 space between the aluminum foil and the roof slab onto which the tile is installed. The brushes  
80 allow sealing the air space perimeter when the tile is supported on wooden battens. Terracotta  
81 tiles are acknowledged to be the finishing layer with underneath ventilation, but the adopted  
82 brushes allow sealing the ventilation layer and exploiting the resulting airspace for thermal  
83 insulation, also thanks to the radiant barrier provided by the aluminum foil. This can largely  
84 offset the loss of the weak cooling effect given by underneath ventilation in summer, while it is

85 however helpful in winter to control heat loss. In fact, a layer of such composite tiles can provide  
86 a strong resistance to heat flow through the roof slab below thanks to the combined action the  
87 insulating layer and the air space. The contribution of the cool color coating is added in summer,  
88 further limiting building overheating and, in combination with that, the negative effects of urban  
89 heat island.

90 The proposed composite tile is intended for installation on uninsulated or poorly insulated  
91 roofs with inhabited spaces below by simply replacing the existing tiles. Thanks to the negligible  
92 increase of thickness, the tile layer can be installed onto an existing roof, for instance the sloped  
93 tile roof of an historical or traditional building, with no need to modify the roof height and  
94 structure, and thus the metal gutters and the other finishing elements that are usually present at  
95 the roof edges or around skylight windows. As a results, an increase of roof insulation is  
96 achieved not far from that provided by a much more invasive installation of a thick insulation  
97 layer, at the same time obtaining a shield against solar radiation more effective than that  
98 provided by the cool color coating alone.

99 The behavior of the developed tile is theoretically and experimentally investigated in this  
100 work, making a comparison with a common tile with the same brick color. Performance  
101 parameter such as solar reflectance, thermal emittance, and thermal conductivity are measured.  
102 Moreover, an experimental test rig has been set up.

103

## 104 **Materials and methods**

105 Experimental data were collected using two painted clay roof tiles. One of the tiles has  
106 been coated by a solar reflective brick red paint with solar reflectance  $\rho_{\text{sol}}=0.46$ , the other one by  
107 a standard paint with the same color but  $\rho_{\text{sol}}=0.22$ . A white basecoat with high solar reflectance  
108 has also been applied to the substrate material before the solar reflective cool color coating in  
109 order to exploit the selective transparency of the coating, if any, and thus further enhance  $\rho_{\text{sol}}$ .  
110 This approach was proposed in [28] and tested in previous work [23-24].

111 The solar reflectance was measured by means of a Devices and Services SSR solar  
112 reflectometer [29] compliant with the ASTM C1549 standard test method [30], using irradiance  
113 spectrum E891BN. The cool colored tile and the standard one were placed onto two battens  
114 mimicking the typical supports for such roof tile. A 2 cm airspace was thus created between the  
115 tile and the base below, consisting of a thick polystyrene panel (Fig. 1). A T-type thermocouple  
116 was placed below the tile, close to its center, to measure the temperature on the bottom surface of  
117 the airspace. In order to control the experimental conditions, another thermocouple was used to  
118 track the evolution of the room temperature during the measurement session. The temperature on  
119 the tile surface was also measured by a FLIR T-640 infrared camera [31]. Moreover, a black  
120 painted aluminum disc with known infrared emittance and an embedded thermocouple was  
121 placed in the field of view of the instrument, properly shielded from the lamp light, in order to  
122 compare the temperature measured by the thermocouple and that measured by the infrared  
123 camera, and thus to detect possible drifts of the surface temperature measurements.

124 All thermocouples were connected to a Pico TC-08 USB thermocouple data logger [32].  
125 Four halogen lamps were placed over the sample and oriented in order to provide an estimated  
126 total irradiance of  $870 \text{ W/m}^2$ , measured by a Delta Ohm HD 9221 radiometer [33]. Since the  
127 instrument is sensitive only in the visible and near infrared range (450-950 nm), the total  
128 irradiance value was extrapolated from the measured one by taking into account the sensitivity  
129 curve of the instrument, the blackbody spectrum of the lamp filament at its nominal temperature  
130 of 4000 K and the transmittance spectrum of the quartz glass protecting the lamps. The obtained  
131 irradiance value is about the peak global irradiance of the sun on a low-slope roof surface in a  
132 typical Mediterranean climate.

133



134  
135  
136

Figure 1. Experimental setup.

137 The experiments consisted of two different stages: in the first one, the tiles were heated by  
138 the lamp system until all temperatures were stabilized, then the lamps were switched off and the

139 surface temperature of the tiles measured by the infrared camera were recorded, as well as the  
140 temperature measured by the thermocouples.

141 In the second stage, the same procedure was followed but an insulating layer was placed  
142 below the cool-colored tile. The insulating layer is made of an aerogel, a silica-gel super-  
143 insulating material, with thickness 1 cm and thermal conductivity 0.015 W/m/K. The thermal  
144 conductivity was verified by a guarded hot plate apparatus available at the University of Modena  
145 and Reggio Emilia. An aluminum foil was also applied below the insulating layer, with thermal  
146 emittance as low as 0.04. This was measured by means of a Devices&Services AE1 thermal  
147 emissometer [34] compliant with the ASTM C1371 standard test method [35]. The surface  
148 without aluminum foil has thermal emittance as high as 0.90. To ensure an almost sealed air  
149 space below the tile, polyester line brushes were attached along the tile perimeter and a  
150 polystyrene frame was also placed around it, in order to avoid transverse heat flux and thus  
151 approach a 1D thermal system.

152 The measured parameters and the used instrumentation are summarized in Tab. 1. The  
153 layer structure of the experimental setup is summarized in Tab. 2.

154

155 |

156

Table 1 – Measured parameters and instruments.

Parameter	Measurement location	Instrument
Solar reflectance	Tile upper surface	D&S SSR solar reflectometer [29-30]
Surface temperature	Tile upper surface, reference disk	FLIR T640 infrared camera [31]
Temperatures	Tile bottom surface, ambient, reference disk	Picotech TC-08 USB datalogger [32] with T-type shielded thermocouples
Irradiance (450-950 nm)	Tile upper surface	DeltaOHM HD9221 photo-radiometer [33]
Thermal emittance	Radiant barrier surface	D&S AE1&RD1 thermal emissometer [34-35]

157

158

Table 2 – Layer structure and materials of the test system.

	Thickness [mm]	Thermal conductivity [W/(m K)]
Tile	10	1.0
Silica aerogel	0-10	0.015
Airspace	20	0.031-0.126*
XPS slab	50	0.040
*equivalent value, calculated with/without radiant barrier		

159

160

161

162

163

164

165

166

167

In brief, the photo-radiometer was used to estimate the irradiance provided by the lamp system. The reflectometer was used to measure the solar reflectance of the tile upper surface and, from that, to estimate the absorbed fraction of the lamp irradiance. The infrared camera was used to measure the temperature of the tile upper surface, acquired immediately after having masked the lamp system in order to avoid measuring also the reflected radiation, and the temperature of the reference disk. The thermocouple system was used to measure the temperature below the tile, the ambient temperature and that of the reference disk. The offset of measurements by the infrared camera with respect to those by the thermocouple system was corrected by comparison

168 of temperatures measured on the reference disk. The combination of temperature measurements  
169 allowed to determine the temperature profile across the tile system.

170 Provided that the brushes effectively seal the thin air space below the tile in either the  
171 described experimental apparatus or the real field application, the air is still in both cases. As a  
172 result, the tile behavior predicted here by theoretical and laboratory analyses can be assumed to  
173 be representative of that of an actual roof in the same ambient conditions.

174

## 175 **Theoretical analysis**

176 A layer of tiles is assumed to be installed on a generic roof with given thermal  
177 transmittance  $U_{roof}$  [W/m<sup>2</sup>/K], that is thermal resistance  $R_{roof} = 1/U_{roof}$  [m<sup>2</sup>K/W], built over a  
178 heated and air conditioned living space. Using a steady-state calculation approach similar to that  
179 outlined in ISO 13790 [36] or already considered in [37-38], the heat flux density  $q$  [W/m<sup>2</sup>]  
180 through the roof surface can be evaluated as follows:

181

$$182 \quad q = [T_e + (1 - \rho_{sol})I_{sol}R_{se} - T_i]/(R + \Delta R) \quad (1)$$

183 where

184  $T_e$  external temperature, given by a combination of air and sky temperatures [°C]

185  $\rho_{sol}$  solar reflectance

186  $I_{sol}$  solar irradiance [W/m<sup>2</sup>]

187  $R_{se}$  surface resistance by convection and infrared radiation [m<sup>2</sup>K/W]

188  $T_i$  internal set point temperature, stabilized by a HVAC system [°C]

189  $R_{roof}$  roof thermal resistance, inverse of the thermal transmittance [ $m^2K/W$ ]  
190  $\Delta R$  increase of the thermal resistance thanks to sub-tile insulation and sealed air gap with  
191 radiant barrier

192

193 The steady state analysis was found to provide a satisfactory agreement with the average  
194 behavior of roof structures typically used in Southern Europe [38]. In steady state, only thermal  
195 resistances must be taken into account, allowing to neglect the actual roof structure with its  
196 thermal masses and inertia.

197 The solar irradiance averaged over the day can be considered for  $I_{sol}$ , or even the peak solar  
198 irradiance. The average irradiance on a surface with given orientation and slope can be  
199 calculated as the ratio the of mean daily irradiation on the same surface and the day length, in  
200 this case obtaining from Eq. (1) the average heat flux in the day. The increase of the roof thermal  
201 resistance  $\Delta R$  can be evaluated as the thermal resistance of the insulation layer attached to the tile  
202 bottom and the sealed air gap below with the radiant barrier provided by the aluminum foil,  
203 reduced by the thermal resistance of the air gap without sub-tile insulation and radiant barrier  
204 (often neglected and so not included in  $R$ ). No condensation/evaporation effects are taken into  
205 account in Eq. (1).

206 The solar reflectance of a cool colored surface can be significantly higher than that of a  
207 conventional surface, but still much lower than a white surface. This is the case of the brick red  
208 surface considered here, whose solar reflectance is increased from 0.22 to 0.46 thanks to the  
209 white basecoat and the cool color coating. However, increasing the roof resistance can have an  
210 effect equivalent to a further increase of solar reflectance. More specifically, for a standard tile

211 without insulation below ( $\Delta R=0$ ) an effective solar reflectance  $\rho_{sol,eff}$  can be calculated, providing  
 212 the same net heat flux density  $q$  of the composite tile with actual reflectance  $\rho_{sol}$  of the cool color  
 213 coating:

$$214 \quad q = [T_e + (1 - \rho_{sol,eff}) I_{sol} R_{se} - T_i] / R \quad (2)$$

216  
 217 Equaling the second terms of Eq. (1) and Eq. (2), and then solving with respect to  $\rho_{sol,eff}$ ,  
 218 one obtains:

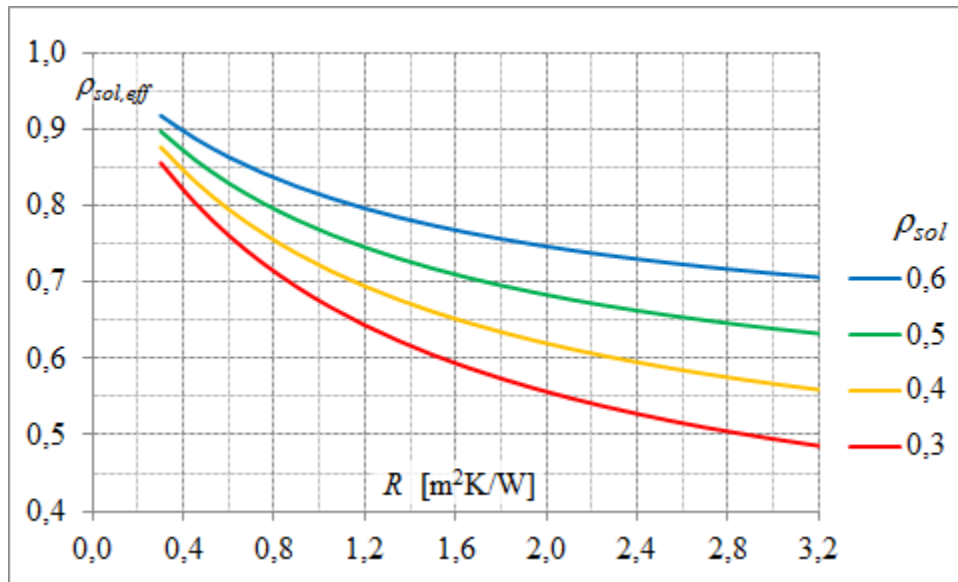
$$219 \quad \rho_{sol,eff} = \rho_{sol} + (1 - \rho_{sol}) \frac{\Delta R}{R + \Delta R} + \frac{[T_e - T_i]}{I_{sol} R_{se}} \frac{\Delta R}{R + \Delta R} \quad (3)$$

221  
 222 The last term in Eq. (3) depends on the local environmental conditions explicitly or  
 223 implicitly expressed by  $T_e$ ,  $I_{sol}$ , and  $R_{se}$ , and the internal set-point temperature  $T_i$ ; such term is  
 224 influenced by the location, the surface orientation, the time in the year and in the day, or even the  
 225 building use. Nonetheless, if  $T_e \geq T_i$ , as it usually occurs in the hot season of Mediterranean areas,  
 226 the last term is always positive and can be conservatively neglected. This leaves the equation  
 227 below for the effective solar reflectance, depending only on the characteristics of roof and tiles:

$$228 \quad \rho_{sol,eff} = \rho_{sol} + (1 - \rho_{sol}) \frac{\Delta R}{R + \Delta R} \quad (4)$$

230

231 The behavior of  $\rho_{sol,eff}$  with respect to the value of  $R$  is plotted in Fig. 2 in order to evidence  
 232 the potential of the composite tile solution.  $\Delta R$  was evaluated according to EN ISO 6946 [39]  
 233 and found equal to  $1.2 \text{ m}^2\text{K/W}$ .  
 234



235  
 236 Figure 2. Effective solar reflectance  $\rho_{sol,eff}$  vs. roof thermal resistance  $R$  and actual solar  
 237 reflectance  $\rho_{sol}$ , for an increase of thermal resistance  $\Delta R = 1.2 \text{ m}^2\text{K/W}$ .  
 238

239 One can observe from Fig. 2 that, for a typical poorly insulated roof with thermal  
 240 resistance around  $1 \text{ m}^2\text{K/W}$ , the roof thermal resistance is more than doubled and an equivalent  
 241 increase of solar reflectance up to a few tens of percentage points is achieved. For a heavily  
 242 insulated roof with thermal resistance around  $3 \text{ m}^2\text{K/W}$ , again an equivalent increase from 0.10  
 243 to 0.20 is achieved, depending on the actual solar reflectance.  
 244

245 A common criticism of cool roofing solutions is related to the loss of solar gains during the  
 246 cold season. A steady state balance of the roof before the refurbishment proposed here can be  
 247 expressed as follows:

$$248 \quad q_{init} = [T_e + (1 - \rho_{sol,init}) I_{sol} R_{se} - T_i] / R \quad (5)$$

250 where

251  $\rho_{sol,init}$  initial solar reflectance before the substitution of the tiles

252  
 253 Subtracting Eq. (1) from Eq. (5) one obtains that no penalization occurs if the result is not  
 254 negative. By proper manipulation of such inequality, one obtains:

$$255 \quad [(\rho_{sol} - \rho_{sol,init}) I_{sol} R_{se}] \leq [T_i - (1 - \rho_{sol,init}) I_{sol} R_{se} - T_e] \Delta R / R \quad (6)$$

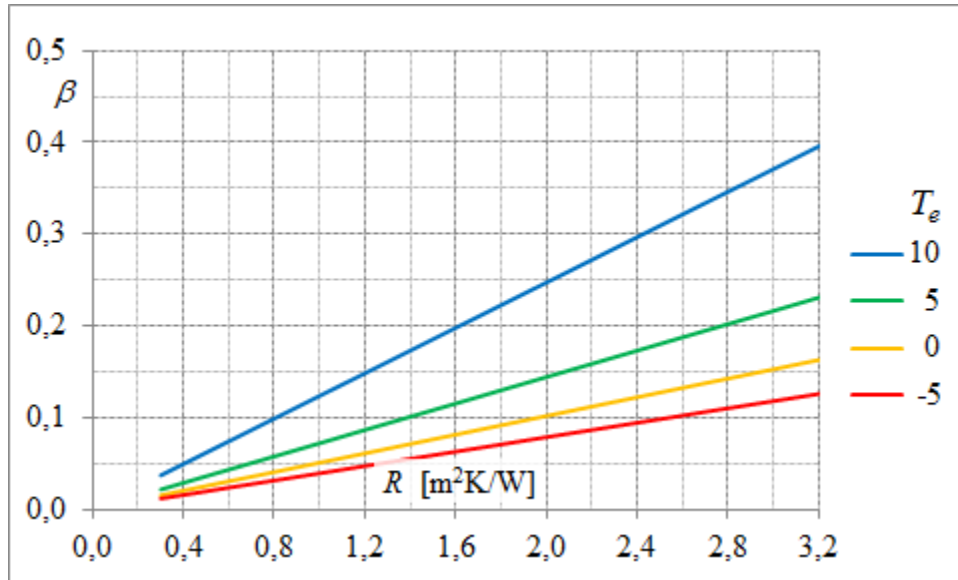
257 or

$$258 \quad \beta = \frac{[(\rho_{sol} - \rho_{sol,init}) I_{sol} R_{se}]}{[T_i - (1 - \rho_{sol,init}) I_{sol} R_{se} - T_e] \Delta R / R} \leq 1 \quad (7)$$

259  
 260 In other words, no penalization exists in the cold season if the loss of solar gains, expressed  
 261 by the left side of Eq. (6), is lower than the reduction of heat loss through the roof, expressed by  
 262 the right side. With an average solar irradiance as low as 100 W/m<sup>2</sup>, typical of Mediterranean  
 263 and sub-Mediterranean areas in the winter months, and surface thermal resistance  $R_{se} = 0.04$   
 264 m<sup>2</sup>K/W as proposed by ISO 6946 [39] for winter heating calculation, as well as  $T_i = 20^\circ\text{C}$ , the

265 ratio  $\beta$  in Eq. (7) is plotted in Fig. 3 for several values of  $T_e$  and  $R$ . One can easily verify that  $\beta$  is  
266 always well below 1.

267



268

269 Figure 3. Ratio  $\beta$  vs. roof thermal resistance  $R$  and external temperature  $T_e$ , for an increase of  
270 thermal resistance  $\Delta R = 1.2 \text{ m}^2\text{K/W}$ .

271

## 272 Experimental results

273 The theoretical analysis was validated through the experiments previously outlined. As  
274 anticipated, steady state conditions were achieved by allowing all temperatures to stabilize.  
275 Significant temperature data recorded by thermocouples and the infrared camera are reported in  
276 Tab. 3.

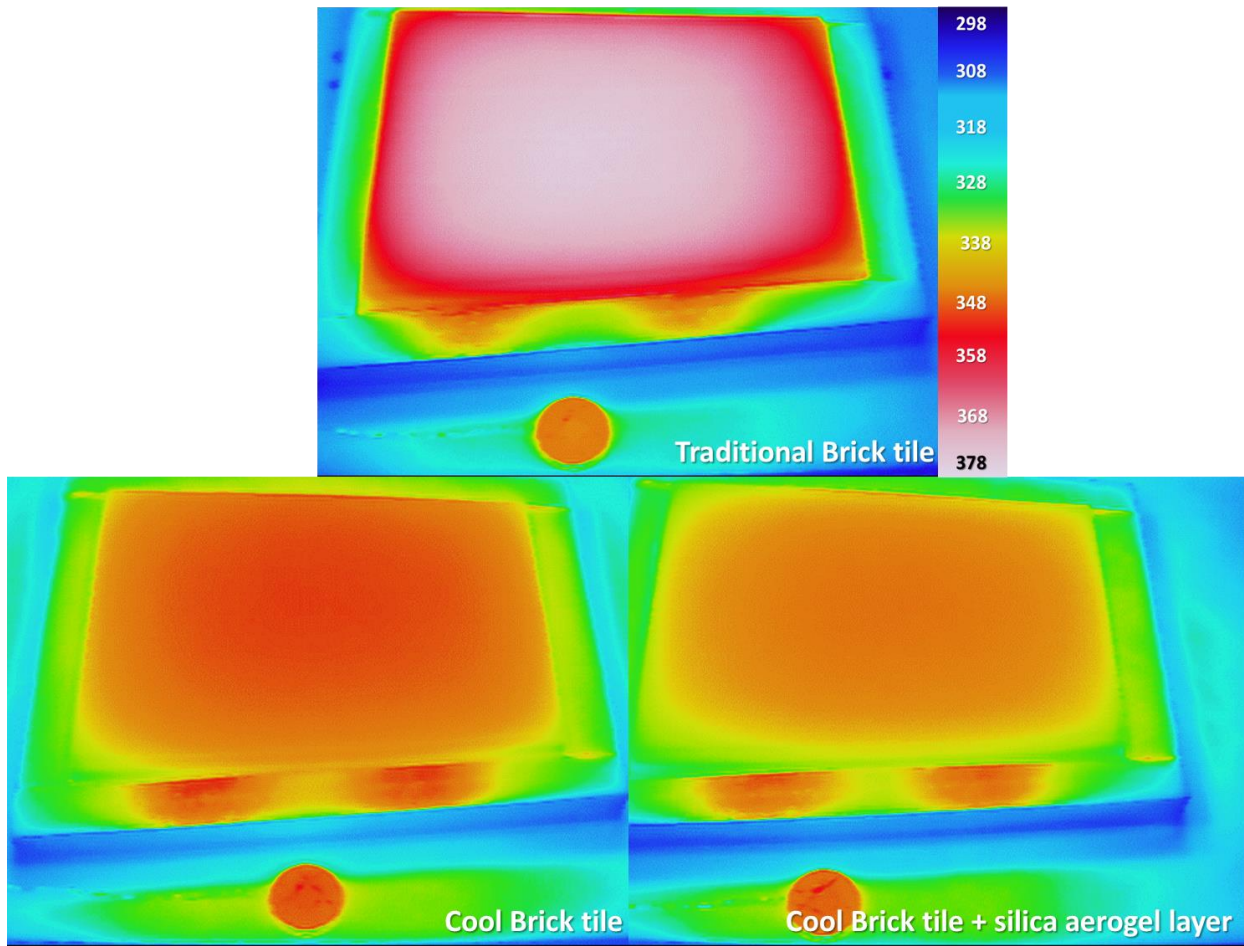
277

278

Table 3 – Measured temperature data.

	Thermocouples		IR camera
	$T_{amb}$ [°C]	$T_{airspace\ bottom}$ [°C]	$T_{tile\ top\ surface}$ [°C]
Standard tile	23.2	74.0	79.5
Cool colored tile	22.5	51.8	60.9
Cool composite tile	21.9	41.5	61.7

279



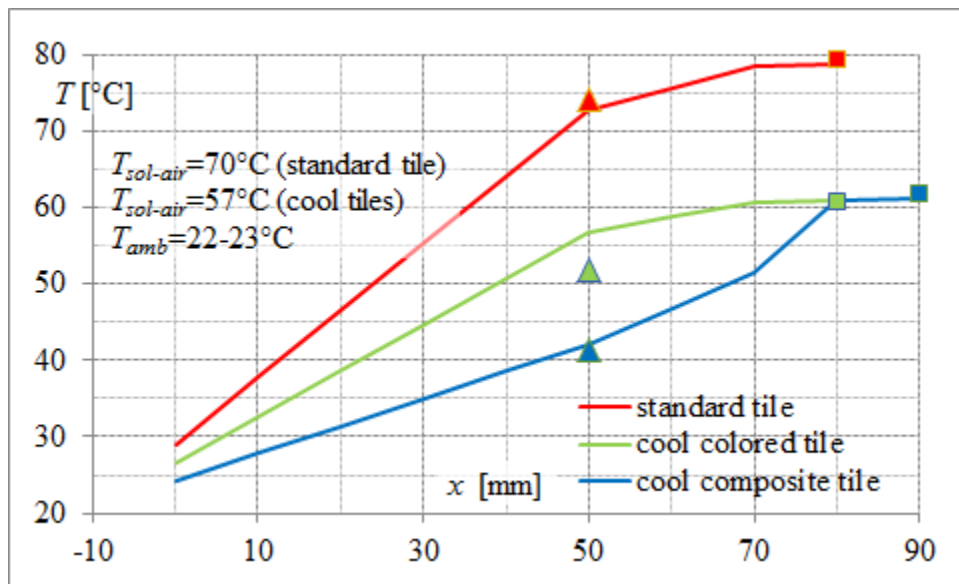
280

281 Figure 4. Infrared thermal images (scalebar in kelvin; the same one was adopted for all pictures).

282

283 Once the temperature was stabilized, the halogen lamp system was switched off and  
 284 quickly masked by an insulating panel in order to prevent any residual irradiation from the light  
 285 source to the measured tile. Immediately after, a thermal picture of the heated tile was acquired

286 by the infrared camera (Fig. 4), from which data reported in Tab. 3 were eventually obtained in  
 287 terms of average surface temperature in an area around the tile center. Contextually, temperature  
 288 measurements from all thermocouples were also acquired. The measured temperature were  
 289 eventually compared to those calculated in steady state (Fig. 5), generally showing a good  
 290 coherence. More specifically, in Fig. 5 continuous lines are temperatures calculated bottom-up  
 291 through the slab-tile thickness, squares are temperatures measured on the tile surface, triangles  
 292 are temperature measured on the airspace bottom surface.  
 293



294  
 295 Figure 5. Comparison of measured temperatures (squares and triangles) and calculated  
 296 temperatures (continuous lines).  
 297

298 Data in Tab. 3 and Fig. 5 show that the cool brick coating alone can provide a sharp  
 299 decrease of both top and bottom surface temperatures with respect to the standard tile. With  
 300 ambient temperature 22-23°C, the maximum temperature on the top surface ( $x=80$  or 90 mm in

301 Fig. 5, marked by squares) decreases from 79.5°C to 60.9°C, while the temperature measured on  
302 the airspace bottom surface ( $x=50$  mm in Fig. 5, marked by triangles) decreases from 74.1°C to  
303 51.8°C. Coupling the cool coated tile with the super-insulating layer and the radiant barrier  
304 below allows a further decrease of the airspace bottom surface temperature to 41.5°C. This  
305 corresponds to an equivalent solar reflectance higher than 0.60, approaching that of a white cool  
306 surface.

307

### 308 **Conclusive remarks**

309 In a Mediterranean architectural context it is quite difficult to integrate cool roofs on  
310 traditional buildings since a good match of roofing colors with the city skyline is generally  
311 required. On the other hand, the actual cool color market can provide building materials which  
312 do not reach very high solar reflectance values, generally below 50%. An interesting solution to  
313 obtain an increase in energy performances can be represented by a coupled system made of a  
314 cool colored roof tile and a thin insulating layer made by silica aerogel and a radiant barrier  
315 below. In this paper, an investigation of such layout is presented and preliminary experimental  
316 results are reported. The results, achieved in steady state condition but to be verified soon by  
317 means of dynamic analysis, showed that a significant improvement can be achieved in terms of  
318 rejection of heat gain, reducing the temperature below the tile layer but at the same time  
319 promoting heat rejection toward the sky by thermal radiation. This effect has been shown to be  
320 mathematically equivalent to an increase of solar reflectance. The cost effectiveness of the

321 proposed approach is also supported by the associated increase of thermal, which is helpful to  
322 decrease heat loss in the cold season.

### 323 **References**

- 324 [1] A.M. Rizwan, L.Y.C. Dennis, C. Liu, A review on the generation, determination and  
325 mitigation of Urban Heat Island, *Journal of Environmental Sciences* 20 (2008) 120-128.
- 326 [2] S. Bretz, H. Akbari, A. Rosenfeld, Practical issues for using solar-reflective materials to  
327 mitigate urban heat islands, *Atmospheric Environment* 32 (1998) 95-101.
- 328 [3] H. Taha, D. Sailor, H. Akbari, High albedo materials for reducing cooling energy use.  
329 Lawrence Berkeley Lab. Rep. 31721 UC-350, 1992.
- 330 [4] S. Konopacki, H. Akbari, L. Gartland, L. (1997). Cooling energy savings potential of light-  
331 colored roofs for residential and commercial buildings in 11 US metropolitan areas, *Energy*  
332 24 (1999) 391–407.
- 333 [5] H. Akbari, M. Pomerantz, H. Taha, Cool surfaces and shade trees to reduce energy use and  
334 improve air quality in urban areas, *Solar Energy* 70 (2001) 295-310.
- 335 [6] Z. Shi, X. Zhang, Analyzing the effect of the longwave emissivity and solar reflectance of  
336 building envelopes on energy-saving in buildings in various climates, *Solar Energy* 85  
337 (2011) 28-37.
- 338 [7] H. Akbari, H.D. Matthews, Global cooling updates: Reflective roofs and pavements,  
339 *Energy and Buildings* 55 (2012) 2-6.

- 340 [8] A. Synnefa, M. Santamouris, Advances on technical, policy and market aspects of cool  
341 roof technology in Europe: The Cool Roofs project, *Energy and Buildings* 55 (2012) 35-  
342 41.
- 343 [9] M. Santamouris, Cooling the cities – A review of reflective and green roof mitigation  
344 technologies to fight heat island and improve comfort in urban environments, *Solar Energy*  
345 103 (2014) 682-703.
- 346 [10] M. Santamouris, C. Pavlou, P. Doukas, C. Mihalakakou, A. Synnefa, A. Hatzibiros, P.  
347 Patargias, Investigating and analysing the energy and environmental performance of an  
348 experimental green roof system installed in a nursery school building in Athens, Greece,  
349 *Energy* 32 (2007) 1781-1788.
- 350 [11] H. Takebayashi, M. Moriyama, Surface heat budget on green roof and high reflection roof  
351 for mitigation of urban heat island, *Building and Environment* 42 (2007) 2971-2979.
- 352 [12] D.J. Sailor, A green roof model for building energy simulation programs, *Energy and*  
353 *Buildings* 40 (2008) 1466-1478.
- 354 [13] H.F. Castleton, V. Stovin, S.B.M. Beck, J.B. Davison, Green roofs; Building energy  
355 savings and the potential for retrofit, *Energy and Buildings* 42 (2010) 1582-1591.
- 356 [14] D.B. Rowe, Green roofs as a means of pollution abatement, *Environmental Pollution* 159  
357 (2011) 2100-2110.

- 358 [15] K.R. Smith, P.J. Roebber, Green roof mitigation potential for a proxy future climate  
359 scenario in Chicago, Illinois, *Journal of Applied Meteorology and Climatology* 50 (2011)  
360 507-522.
- 361 [16] S.W.Tsang, C.Y. Jim, Theoretical evaluation of thermal and energy performance of  
362 tropical green roofs, *Energy* 36 (2011) 3590-3598.
- 363 [17] M. Zinzi, S. Agnoli, Cool and green roofs. An energy and comfort comparison between  
364 passive cooling and mitigation urban heat island techniques for residential buildings in the  
365 Mediterranean region, *Energy and Buildings* 55 (2012) 66-76.
- 366 [18] R. Levinson, P. Berdahl, H. Akbari, Solar spectral optical properties of pigments—Part I:  
367 model for deriving scattering and absorption coefficients from transmittance and  
368 reflectance measurements, *Solar Energy Materials and Solar Cells* 89 (2005) 319-349.
- 369 [19] R. Levinson, P., Berdahl, H. Akbari, Solar spectral optical properties of pigments—Part II:  
370 survey of common colorants, *Solar Energy Materials and Solar Cells* 89 (2005) 351-389.
- 371 [20] M. Santamouris, K. Pavlou, A. Synnefa, K. Niachou, D. Kolokotsa, Recent progress on  
372 passive cooling techniques. Advanced technological developments to improve survivability  
373 levels in low-income households, *Energy and Buildings* 39 (2007) 859-866.
- 374 [21] A. Synnefa, M. Santamouris, H. Akbari, Estimating the effect of using cool coatings on  
375 energy loads and thermal comfort in residential buildings in various climatic conditions.  
376 *Energy and Buildings* 39 (2007) 1167-1174.

- 377 [22] A. Synnefa, M. Santamouris, K. Apostolakis, On the development, optical properties and  
378 thermal performance of cool colored coatings for the urban environment, *Solar Energy* 81  
379 (2007) 488-497.
- 380 [23] A. Libbra, L. Tarozzi, A. Muscio, M.A. Corticelli, Spectral response data for development  
381 of cool coloured tile coverings. *Optics & Laser Technology* 43 (2011) 394-400.
- 382 [24] A. Libbra, A. Muscio, C. Siligardi, P. Tartarini, Assessment and improvement of the  
383 performance of antisolar surfaces and coatings, *Progress in Organic Coatings* 72 (2011) 73-  
384 80.
- 385 [25] A.L. Pisello, F. Cotana, A. Nicolini, L. Brinchi, Development of clay tile coatings for  
386 steep-sloped cool roofs, *Energies* 6 (2013) 3637-3653.
- 387 [26] C. Ferrari, A. Libbra, A. Muscio, C. Siligardi, Design of ceramic tiles with high solar  
388 reflectance through the development of a functional engobe, *Ceramics International* 39  
389 (2013) 9583-9590.
- 390 [27] C. Ferrari, A. Muscio, C. Siligardi, T. Manfredini, Design of a cool color glaze for solar  
391 reflective tile application, *Ceramics International* (2015) in press,  
392 doi:10.1016/j.ceramint.2015.05.058.
- 393 [28] R. Levinson, H. Akbari, P. Berdahl, K. Wood, W. Skilton, J. Petersheim, A novel  
394 technique for the production of cool colored concrete tile and asphalt shingle roofing  
395 products. *Solar Energy Materials & Solar Cells* 94, 946-954.

- 396 [29] Devices&Services Company, SSR – Solar Spectrum Reflectometer Model SSR,  
397 <http://www.devicesandservices.com/prod01.htm>.
- 398 [30] ASTM, C1549-09 – Standard Test Method for Determination of Solar Reflectance Near  
399 Ambient Temperature Using a Portable Solar Reflectometer, 2009, <http://www.astm.org>.
- 400 [31] FLIR, FLIR T620 & T640 Datasheet (rev 06/12), 2012, [www.flir.com](http://www.flir.com).
- 401 [32] Pico Technology, TC-08 Thermocouple Data Logger – Specifications, 2013,  
402 [www.picotech.com](http://www.picotech.com).
- 403 [33] Delta OHM, HD 9221 Photo-radiometer – Instructions Manual, [www.deltaohm.com](http://www.deltaohm.com).
- 404 [34] Devices&Services Company, AE1 & RD1 – Emissometer with Scaling Digital Voltmeter  
405 Model AE1 RD1, <http://www.devicesandservices.com/prod03.htm>.
- 406 [35] ASTM (ASTM International) 2010. ASTM C1371-04a(2010)e1 – Standard Test Method  
407 for Determination of Emittance of Materials Near Room Temperature Using Portable  
408 Emissometer, 2013, <http://www.astm.org>.
- 409 [36] ISO 13790:2008 – Energy performance of buildings – Calculation of energy use for space  
410 heating and cooling, 2008.
- 411 [37] R. Levinson, H. Akbari, J.C Reilly, Cooler tile-roofed buildings with near-infrared-  
412 reflective non-white coatings, *Building and Environment* 42 (2007), 2591-2605.

- 413 [38] A. Libbra, A. Muscio, C. Siligardi, Energy performance of opaque building elements in  
414 summer: Analysis of a simplified calculation method in force in Italy, Energy and  
415 Buildings 64 (2013) 384-394.
- 416 [39] ISO 6946:2007 – Building components and building elements – Thermal resistance and  
417 thermal transmittance – Calculation method, 2007.